

## MULTI-CHANNEL LIDAR SPECTROMETER FOR ATMOSPHERIC AEROSOL TYPING ON THE BASIS OF CHEMICAL SIGNATURES IN RAMAN SPECTRA

Boyan Tatarov<sup>1</sup>, Nobuo Sugimoto<sup>1</sup>, Ichiro Matsui<sup>1</sup>, Dong-Ho Shin<sup>2</sup>, Detlef Müller<sup>2,3</sup>

<sup>1</sup> National Institute for Environmental Studies, 16-2 Onogawa, Tsukuba, Ibaraki, Japan,  
E-mail: boyan.tatarov@nies.go.jp

<sup>2</sup> Atmospheric Remote Sensing Laboratory, Gwangju Institute of Science and Technology (GIST),  
1 Oryong-dong, Buk-Gu, Gwangju 500-712, Republic of Korea, E-mail: detlef@gist.ac.kr

<sup>3</sup> Leibniz Institute for Tropospheric Research, Permoser Str. 15, 04318 Leipzig, Germany, E-mail: detlef@tropos.de

### ABSTRACT

We present a first experimental data on chemical signatures characteristic for trace gases or particulate pollution (aerosol types). Measurements were made with a system that is based on a combination of a multi-channel spectrometer and a High Spectral Resolution Lidar. Measurements were also made with a combination of the multi-channel spectrometer and a multi-wavelength Raman lidar.

### 1. INTRODUCTION

In inelastic Raman scattering the scattered signal consists of radiation that has undergone a frequency shift which is characteristic for the stationary energy states of an irradiated molecule [1]. Nowadays, Raman spectroscopy is commonly used in chemistry. Information on the radiation that results from transition between the vibrational energy states of the excited molecules, respectively, is specific to the chemical bonds and symmetry of molecules. This radiation therefore provides unique information regarding the irradiated molecule according to which the molecular species can be identified. Raman spectroscopy represents a particularly powerful tool for laser remote sensing because it allows us to both identify and quantify the trace constituent relative to the major constituents of a mixture. Raman lidar systems have become wide-spread. At the moment these systems allow for an independent quantitative measurement of the aerosol backscatter and extinction coefficient profiles on the basis of Raman scattering from nitrogen or oxygen molecules [2]. However, for a better understanding of the radiative impact of atmospheric aerosol pollution we need in future lidar measurement techniques that allow for an identification of different aerosol types, as for instance desert dust, urban haze, forest fire smoke, etc.

In our previous study we proposed a method to estimate the concentration of mineral dust by using lidar return signals from Raman scattering of quartz (silicon dioxide, silica), which is the major constituent of mineral dust [3]. This method combines the Raman scattered quartz signature at  $466\text{ cm}^{-1}$  with a High-

Spectral-Resolution Lidar (HSRL) to estimate the quartz concentration in the atmospheric aerosols.

In this paper we present a multi-channel spectrometric lidar system which allows us to measure Raman spectrums that give us information on chemical signatures characteristic for chemical components (trace gases) of aerosol particles. In the following, we describe the system and we show first experimental results.

### 2. METHODS AND APPARATUS

The multi-channel lidar system used in our study works on the basis of the high-spectral-resolution techniques. The system has been developed at the National Institute for Environmental Studies (NIES) [4]. The lidar system was modified with a Licel Multispectral Lidar Detector. The detector allows for the simultaneous detection of

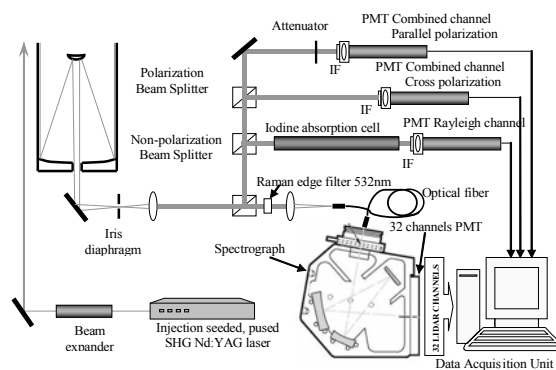


Figure1. Scheme of the lidar system.

multiple spectrometer wavelengths. The spectrometer is based on a spectrograph and a Hamamatsu H7260-20 multianode, metal-channel-dynode photomultiplier with 32 photocathode elements. The detector is supplied with 32 single photon-counting systems, which provide 2-dimensional data, i.e., we obtain range-resolved signals, which in addition are separated according to the wavelength. The spectrograph is an F/3.7 Crossed Czerny-Turner ORIEL MS125 - 77400, with 120 mm focal length. For this work two different gratings were used – one is 1200 lines/mm that secure spectral resolution of about  $\Delta\lambda\sim 6\text{nm}$  and a second grating with 1800 lines/mm ( $\Delta\lambda\sim 4\text{nm}$ ).

The diagram of the system is shown in Figure 1. A detailed description of the HSRL part is presented in [4]. The measurement wavelength of the HSRL was set to  $\lambda_L=532.24$  nm ( $18\,788.451$  cm<sup>-1</sup>). In its current design 70% of the backscattered signal are used for the multi-spectral Raman observations and 30% are used for the HSRL/polarization observations. An optional Raman edge filter was used to reduce the high intensity elastic signal that enters the multi-spectral detector. The optical filter is characterized by an optical density of  $\sim 7$  for the laser line at  $\lambda_L=532.24$  nm and an averaged pass band transmission of more than 93% for wavelengths from 537 to 736 nm. The system allows us to measure simultaneously and independently vertical profiles of Raman backscatter at 32-channels, the particle extinction coefficient, the particle backscattering coefficient, and the total (volume) depolarization ratio. The lidar ratio, the optical depth, the backscattering ratio and the (linear) particle depolarization ratio follow from these measurements.

The Raman backscatter signals obtained by the spectrometer are described by the Raman lidar equations and can be written as [2]:

$$P_{R_i}(r, \lambda_L, \lambda_{R_i}) = P_L \frac{B_R F_R(r)}{r^2} \beta_{R_i}(r, \lambda_L, \lambda_{R_i}) \times \exp\left(-\int_0^r [\alpha_p(z, \lambda_L) + \alpha_m(z, \lambda_L) + \alpha_p(z, \lambda_{R_i}) + \alpha_m(z, \lambda_{R_i})] dz\right) \quad (1),$$

where  $i=1,2,\dots,32$  is the number of the channel,  $P_{R_i}(r, \lambda_L, \lambda_{R_i})$  is the power received from distance  $r$  at the Raman wavelength  $\lambda_{R_i}$ ,  $P_L$  and  $\lambda_L$  are the power and wavelength of the transmitted light,  $F(r)$  is the geometrical form factor of the transmitter/receiver system,  $B$  is a constant that includes all range independent parameters, and  $\beta_{R_i}(r, L, \lambda_{R_i})$  are the Raman backscatter coefficients. The extinction coefficients are denoted by  $\alpha_p$  for aerosol particles and  $\alpha_m$  for atmospheric gaseous molecules.

The Raman backscatter coefficients  $\beta_{R_i}(r, \lambda_L, \lambda_{R_i})$  of the scatterers at all wavelengths can be determined from the received Raman scattering signal based on the knowledge of the system parameters ( $B$  and  $F(r)$ ) and the optical depth of the atmosphere. Aerosol extinction (respectively optical depth) and backscatter coefficients at the laser wavelength can be obtained by simultaneous HSRL observations or Raman lidar signals obtained with the spectrometer for pure rotational Raman, signals from nitrogen molecules.

In this way, the concentration of the atmospheric components can be estimated based on the Raman backscatter coefficient for the individual wavelengths. For instance the relation of the Raman backscatter

coefficient with the Raman backscatter differential cross section  $d\sigma(\lambda_L, \lambda_{R_i}, \pi)/d\Omega$  and the number density of quartz molecules  $N_{qi}$  can be used for such a purpose. The relation is defined by the expression:

$$\beta_{R_i}(r, \lambda_L, \lambda_{R_i}) = N_{qi}(r) \frac{d\sigma(\lambda_L, \lambda_{R_i}, \pi)}{d\Omega}. \quad (3)$$

### 3. RESULTS AND DISCUSSION

#### 3.1 Simultaneous detections of Raman lines of pure-rotational, N<sub>2</sub>, O<sub>2</sub>, H<sub>2</sub>O and elastic signal

An example of data obtained by the multi-spectral lidar detector on 6 February, 2009 is shown in Figure 2. The lidar is operated at the National Institute for

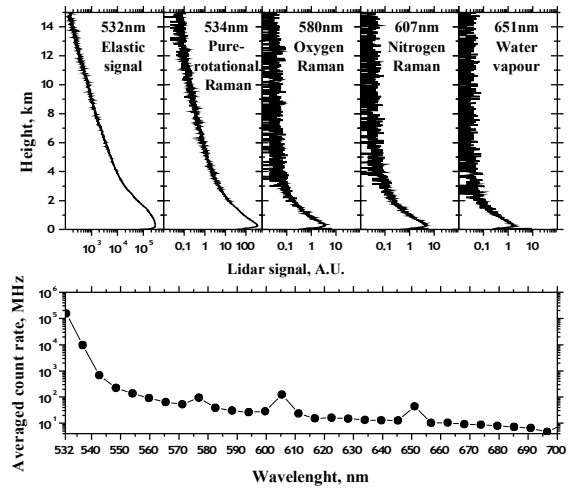


Figure 2. Vertical profiles of elastic and Raman lidar signals (upper panels) and raw spectra (bottom panel) averaged across the vertical range from 100m to 2000m. Measurement time was from 1009-1057 UTC on 6 February 2009.

Environmental Studies (NIES), Tsukuba, Japan ( $36.05^\circ$  N,  $140.12^\circ$  E, 27 m above sea level). Lidar signals were recorded from 1009 to 1057 UTC with a 10 Hz repetition rate (28800 laser shots). The vertical resolution is 15 m, the spectral resolution is  $\Delta\lambda=5.7$ nm. The bottom panel of the figure represents the spectrum of the backscattered radiation in the vertical range from 100 m to 2000 m. In this spectrum, we can identify several peaks: the Mie (elastic) scattering at 532nm, the Raman scattering from oxygen molecules at 580nm ( $1556$  cm<sup>-1</sup>), the Raman scattering from nitrogen molecules at 607nm ( $2331$  cm<sup>-1</sup>), and the Raman scattering from water molecules at 651nm ( $3652$  cm<sup>-1</sup>). The vertical profiles of the lidar returns from these major components are presented in the upper panels of Figure 2.

### 3.2 Observations of mineral dust over Tsukuba

Figure 3 presents a measurement example of a mineral dust episode that occurred on 17 March 2009. A large mineral dust plume was transported over the lidar site on this day. We took data with our multi-spectral Raman lidar detector that was installed in the HSRL. We also carried out particle polarization measurements. The presence of the dust plume over this part of Japan was confirmed by independent measurements of the polarization lidars of the NIES Lidar Network [5].

Lidar signals were recorded from 1105 to 1745 UTC (240000 laser shots). The vertical resolution of the profiles is 150 m, the spectral resolution is  $\Delta\lambda=3.5\text{nm}$ .

altitude above ground. The vertical profile of the total linear (volume) depolarization ratio has relatively high values in the altitude range up to 9 km, namely, about 20 % depolarization between 0.5 km and 3 km, and up to 8 % linear depolarization in heights from 3 km to 8 km. The high depolarization ratios indicate scattering from particles with non-spherical shape.

We find enhanced signal levels in the 545.8-nm Raman channel between 3 km and 9 km height. This channel corresponds to the quartz Raman line at  $466\text{cm}^{-1}$  [3]. Elevated values of Raman signals in that same altitude range can also be seen in the 549.3 nm channel ( $584\text{cm}^{-1}$ ). Most probably, the enhanced signal level

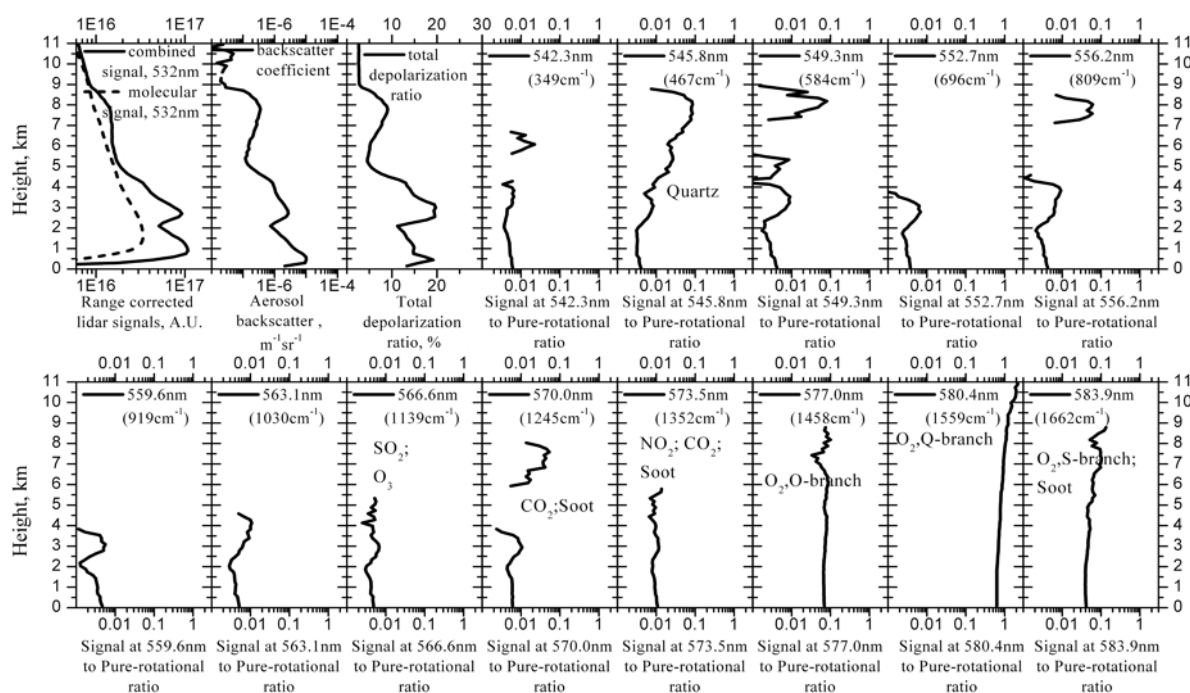


Figure 3. Vertical profiles of lidar return signals at different detection wavelengths during the advection of a mineral dust plume observed from 1105 to 1745 UTC on 17 March, 2009.

All vertical profiles of the different inelastic Raman signal components are background subtracted, range corrected and normalized to the pure-rotational Raman signal obtained at the channel with central wavelength 534 nm ( $\Delta\lambda=3.5\text{nm}$ ). In this figure we only present the portions of the profiles of the Raman signals that are characterized by signal-to-noise ratios higher than 1, respectively. The molecular part of the optical profiles is obtained from radiosonde observations which are carried out on a routine basis at the Tateno Aerological Observatory ( $36.05^\circ\text{N}$ ,  $140.13^\circ\text{E}$ ).

The profile of the aerosol backscatter coefficient shows the presence of several aerosol layers up to 9 km

corresponds to Raman scattering from other silicate components or specific structures (lattice) of the quartz crystals. Increased levels of the Raman signals in the height range of the dust plume (up to about 3 km) are also observed at 552.7 nm, 556.2 nm, 559.6 nm, and 570.0 nm. The signal at 566.6 nm can be related to Raman scattering from sulphur dioxide (Raman line  $1151\text{cm}^{-1}$ ) and/or ozone (Raman line  $1103\text{cm}^{-1}$ ). Raman scattering of soot could result in lidar return signals at 570.0 nm and 573.5 nm (Raman soot line  $1331\text{cm}^{-1}$ ) as well as at 583.9 nm (Raman soot line  $1600\text{cm}^{-1}$ ). The Raman scattering of oxygen dominates at three channels - 577.0nm (O-branch), 580.4nm (Q-branch) and 583.9nm (S-branch).

### 3.3 Raman and fluorescence spectrum measured in the boundary layer over Gwangju

Figure 4 shows first results of measurements with the spectrometer installed into the multiwavelength Raman lidar of the Gwangju Institute of Science and

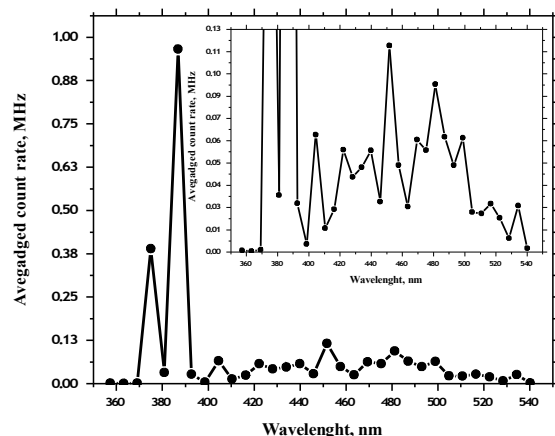


Figure 4. Raman and fluorescence spectrum averaged in the height range from 150 m to 300 m. The measurement was carried out at Gwangju from 11:42 to 15:40 UTC on 27 November 2009.

Technology (GIST) in South Korea. This aerosol Raman lidar system provides particle backscatter coefficients at 355, 532, and 1064 nm, and extinction coefficients at 355 and 532 nm. The combination of optical data allows us to separate among different aerosol types. Inversion algorithms [6, 7] can be used to infer microphysical particle parameters. In this sense, the upgrade of the system with a spectrometer could add extremely valuable information as the Raman spectra contain chemical signatures of chemical components characteristic of specific aerosol types of aerosol particulate pollution, like for instance Asian dust (silicates), forest-fire smoke (soot) and urban haze (sulphur dioxide, nitrous oxide, soot).

Disadvantage of the GIST lidar system is the comparably low laser output energy. The cooperation between NIES and GIST therefore offers an excellent opportunity of testing the concept of the spectrometer (powerful HSRL at NIES) with the aerosol typing capabilities of a state-of-the art multiwavelength Raman lidar (at GIST).

The laser wavelength 355 nm was chosen as pumping wavelength for the spectrometric observations, which offered us the chance to test the spectrometer in the UV. Our first measurements show that the GIST system is capable of detecting the main atmospheric gases at 376 nm (oxygen) and 387 nm (nitrogen) as well as Raman scattering of water vapor at 407 nm.

We find a broad spectrum of lidar return signals between 400 and 540 nm. The general shape of this spectrum points to fluorescence. However, we see several peaks on top of this broad spectrum. At the moment it is not clear to us if these peaks are artefacts or if they are linked to signals from different chemical components. We are currently searching in data bases (e.g. atomic emission spectroscopy) for explanations of these peaks.

### 4. SUMMARY

We present first measurements of various chemical components (mineral quartz, sulphur dioxide) with a novel spectrometer. The measurements show that in principle it is possible to identify chemical components in particulate pollution in terms of chemical signatures contained in Raman spectra of the atmosphere. These measurements were carried out with a powerful High-Spectral-Resolution-Lidar at NIES in Tsukuba, Japan. The spectrometer was subsequently installed into the multiwavelength aerosol Raman lidar at the Gwangju Institute of Science and Technology (GIST) in South Korea. Goal of the cooperation between NIES and GIST is to show if an identification of chemical components in particulate pollution can help in improving the optical and microphysical aerosol typing of the complicated pollution situation over East Asia.

### 5. ACKNOWLEDGMENTS

This work has been primarily supported by the Ministry of the Environment, Tokyo, Japan. Work at GIST is funded by the Korea Meteorological Administration Research and Development Program under Grant CATER 2009-3112.

### REFERENCES

- [1] Measures, R. M., Laser Remote Sensing, 510 pp., John Wiley, New York, 1984
- [2] Ansmann, A., Riebesell, M., and Weitkamp, C.: Measurement of atmospheric aerosol extinction profiles with a Raman lidar, *Opt. Lett.* 15, 746-748, 1990.
- [3] Boyan Tatarov and Nobuo Sugimoto, "Estimation of quartz concentration in the tropospheric mineral aerosols using combined Raman and high-spectral-resolution lidars," *Opt. Lett.* 30, 3407-3409 (2005)
- [4] Z. Liu, I. Matsui, and N. Sugimoto, *Opt. Eng.* 38, 1661, (1999)
- [5] A. Shimizu, N. Sugimoto, I. Matsui, K. Arao, I. Uno, T. Murayama, N. Kagawa, K. Aoki, A. Uchiyama, and A. Yamazaki, *J. Geophys. Res.* 109, S17 (2004).
- [6] Müller D., et al., Microphysical Particle Parameters From Extinction and Backscatter Lidar Data by Inversion With Regularization: Theory, *Appl. Opt.*, Vol. 38, 2346 - 2357 (1999).
- [7] Veselovskii, I. et al., Inversion With Regularization for the Retrieval of Tropospheric Aerosol Parameters From Multiwavelength Lidar Sounding, *Appl. Opt.*, Vol. 41, 3685-3699 (2002).